CFD Assessment of Thermal Comfort and Indoor Air Quality Using Ductless Personalized Ventilation

Hayder Alsaad and Conrad Voelker
Department of Building Physics, Bauhaus-University Weimar
Weimar, Germany
hayder.alsaad@uni-weimar.de, conrad.voelker@uni-weimar.de

Abstract

Computational Fluid Dynamics (CFD) simulations were used to study the thermal environment and indoor air quality in a room equipped with Displacement Ventilation (DV) and a Ductless Personalized Ventilation system (DPV). In order to validate the model, a series of empirical measurements were executed in a climate chamber equipped with a thermal manikin, a tracer gas system, and a set of air temperature and velocity sensors. Data collected from measurements were used to develop the numerical model. Results from the numerical model were then used to quantify thermal comfort and sensation using UC Berkeley thermal comfort model. Results show that indoor air quality -expressed using the ventilation effectiveness index- was improved by up to 0.98 when DPV was used. Furthermore, UC Berkeley model simulations showed a possibility of improving thermal comfort by up to 2.24 points on the thermal comfort scale.

Introduction

Humankind invented buildings to yield security and shelter from bad weather. Humans spend most of their day in these buildings. Therefore, attention must be paid to their quality (Zeng & Zhao, 2005). Thermal discomfort and low indoor quality highly affects occupants' health and performance (Wyon & Wargocki, 2006a, 2006b). Buildings are equipped with mechanical Heating, Ventilation and Air Conditioning (HVAC) systems to maintain a sufficient level of thermal comfort and indoor air quality. These systems control the physical environmental factors reported by Fanger (1970) that affect human comfort, such as air temperature, air velocity, and relative humidity. However, total volume ventilation systems that are commonly used in building nowadays treat the whole volume of the space which consumes a significant amount of energy (Lipczynska, Kaczmarczyk, & Melikov, 2014).

Displacement ventilation (DV) is a total-volume system that delivers the outdoor air into the room with low velocity from an inlet located near the floor and extracting it using an outlet located near the ceiling (Skistad & Mundt, 2002). This system creates a vertical stratification due to the buoyancy forces generated by the heat sources in the room. Thus, the fresh cool air at the bottom of the space moves upwards through the thermal plumes of the heat sources, removing heat and contaminants to the upper layer of the air in the space (Abbas, 1999). Even though DV provides better air quality than typical mixing ventilation systems (Skistad & Mundt, 2002), it lacks the individual control that complies with the personal preference of each occupant (Gao & Niu, 2004). Furthermore, studies show that the indoor air quality using DV is affected by many factors such as the location of the pollutants source or walking people around the occupant (Halvoňová & Melikov, 2010a).

Personalized ventilation has been suggested to improve the indoor environment (Fanger, 2001). Personalized ventilation (PV) is a system that provides fresh air to the occupant's breathing zone. It allows individual control over air velocity, direction, and possibly temperature too (Melikov, 2004). Thus, unlike axial fans, PV systems target both thermal comfort and indoor air quality. Researchers have investigated the performance of PV under various setups using human subjects (Kaczmarczyk, Melikov, Bolashikov, Nikolaev, & Fanger, 2006; Kalmár & Kalmár, 2013; Yang, Sekhar, & Melikov, 2010), or thermal manikins (Bolashikov, Melikov, & Krenek, 2010; Conceição et al., 2010; Lipczynska, Kaczmarczyk, & Melikov, 2015), or Computational Fluid Dynamics (CFD) (He, Niu, Gao, Zhu, & Wu, 2011; Russo & Khalifa, 2010; Shen, Gao, & Wang, 2013). Results indicate that PV always improves the indoor environment, in both heating and cooling seasons (Chludzińska & Bogdan, 2015). Recent research shows that even implementing PV alone without being combined with another ventilation system can achieve the same level of air mixing and air-change effectiveness in the occupied space (Lipczynska et al., 2015).

PV systems are typically connected to a duct that supplies fresh tempered air from the outdoor, which significantly increases the ductwork of a project. Furthermore, it restricts the arrangement of furniture in the room and affects its aesthetics. Therefore, a ductless personalized system was suggested (Dalewski, Melikov, & Vesely, 2014). Ductless Personalized Ventilation (DPV) is a mean of bringing cool fresh air from the lower level of the room and delivering it directly to the occupants face. It is used in combination with Displacement Ventilation (DV) due to the vertical stratification created by this ventilation system (Halvoňová & Melikov, 2010b). In order to avoid transporting pollutants from the floor level to the occupants face region and to enhance the perceived air quality, it is recommended to install a filter at the intake of the system (Dalewski, Vesely, & Melikov, 2012).

https://doi.org/10.26868/25222708.2017.076

Dalewski et al. (2014) investigated the performance of DPV using human subjects. It was found that using DPV in combination with DV improves perceived indoor air quality especially in warm environments (29°C). Thermal comfort was also improved when the systems combination was used with indoor air temperature higher than 23°C. Chakroun et al. (2011) researched the performance of a DV system coupled with chilled ceiling and a ductless evaporative system that implements a wet pad to cool the air that is being drawn from the lower layer of the room air. Results show that the system can achieve the same level of thermal comfort when the supply air temperature is higher by 3 K than the supply air temperature of DV alone. Ghaddar, Ghali, and Chakroun (2013) investigated the performance of the same system, yet under transient conditions. It was found that when undersizing the HVAC system by 25%, transient thermal discomfort was eliminated using the ductless evaporative system even with a temperature drift of 3.9°C.

This research consists of two parts: empirical measurements and computer simulations. Computer simulation was used to investigate the indoor environment and to quantify thermal sensation and thermal comfort. The aim is to assess the performance of DPV by comparing the thermal environment and indoor air quality under various boundary conditions in two scenarios; DV alone and DV combined with DPV.

Methods

Experimental apparatus

Empirical measurements were performed in a 3 x 3 x 2.44 m climate chamber situated in a laboratory hall (5.40 x 5.40 x 3.05 m) to keep it isolated from the outdoor environment. The chamber is tempered by water-bearing capillary tubes placed under the finishing layer (tiles for the floor and gypsum plaster for walls and ceiling). The temperature in the chamber can be set between 10-40°C by controlling the temperature of each surface separately, or by setting the temperature of the ventilation system, or both. The chamber utilizes two inlets to introduce fresh or recirculated air in an adjustable rate into the chamber. Inlets are located at one of the corners of the chamber (Figure 1), they each consist of a set of 6 pipes with a diameter of 4.5 cm. Concurrently, the system utilizes two outlets with the same dimensions and properties as the inlets. These outlets are located at the opposite corner of the inlets. For this research, only the lower inlet and the upper outlet were utilized to create a displacement ventilation system.

The climate chamber is equipped with a thermal manikin with complex male body shape that simulates the thermal attributes of a human body. The manikin is 1.68 cm height in the standing position and 1.23 cm in the upright sitting posture (Figure 1). The manikin body consists of 22 body segments; the temperature of each body segment can be controlled separately through heating nickel wires embedded under the manikin's surface. The manikin temperature can be set to resemble the thermal attributes of a human body in a comfortable state, or it can be manually set between 18 – 42°C with a precision of ±0.2°C.

Negative temperature coefficient thermistors (NTC) with an accuracy of ±0.1K of the measured values were used along with hot-wire omni-directional anemometers with an accuracy of ±1.5% of the measured values in order to evaluate the thermal environment in the climate chamber. Indoor air quality was evaluated by measuring tracer gas concentrations in the chamber. INNOVA 1303 multipoint sampler and doser was used to constantly dose CO_2 in the chamber through the manikin's mouth. Tracer gas concentrations were measured using INNOVA 1412 photoacoustic gas monitor with a CO_2 detection accuracy of ±2% of the measured concentration. The tracer gas system was located outside the chamber, air samples were withdrawn into the photoacoustic gas monitor using nylon tubing.

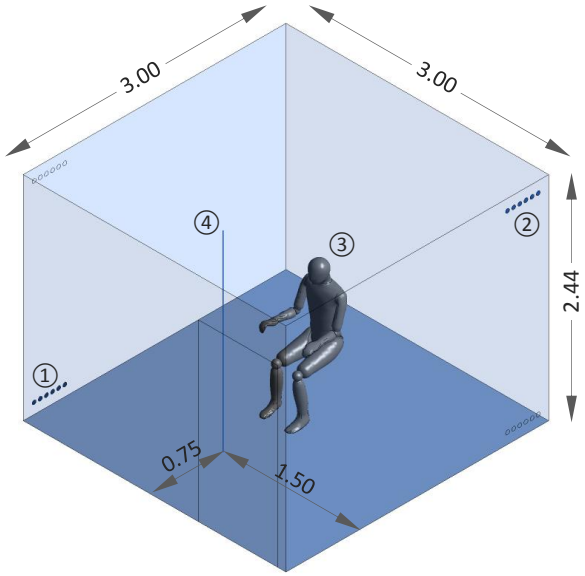

Figure 1: The climate chamber: (1) supply inlet, (2) exhaust outlet, (3) thermal manikin, (4) vertical measurements bar. Dimensions are in meters.

Experimental setup

The experimental study was conducted under two supply air temperature settings: θ_s = 19°C and 22°C. The ventilation flow rate of the climate chamber was set to $\dot{V}$ = 16, 24, and 43 l/s with each air temperature setting, thus a total of 6 experimental setups (*16 l/s_19°C, 24 l/s_19°C, 43 l/s_19°C, 16 l/s_22°C, 24 l/s_22°C,* and *43 l/s_22°C*). All the surfaces of the chamber were turned off. Hence, the chamber was tempered using only the ventilation system.

The manikin was set to comfort mode and placed approximately at the center of the chamber. Since results from the empirical measurements were intended to validate the numerical model, empirical measurements were performed using a bald, naked manikin placed on an open office chair in order to simplify the numerical model. For the same reason, the respiratory system of manikin was turned off and replaced with a constant flow of CO_2

through the mouth to simulate an active contamination source. CO_2 was dosed with a flow rate of $\dot{V}_{gas}$ = 3 ml/s, no tracer gas was added to the air supplied to the chamber. Supply air was set to fresh air rather than recycled air in order to control the tracer gas measurements. Relative humidity was around 45-60% depending on the outside relative humidity.

Before each experiment, the chamber was constantly monitored and given enough leading time to reach a thermal steady state. After steady state was achieved, data were recorded for 1 hour for each experimental setup. Temperature and velocity measurements were recorded with a sampling interval of t = 10 seconds and averaged. Vertical gradients of velocity, temperature, and tracer gas concentration were measured at the same location by mounting all of the sensors and the tubes of the gas monitor on one vertical metal bar (Figure 1). Hot-wire anemometers were mounted at 0.20, 0.40, 0.60, 0.80, 1.10, 1.60, and 2.10 m height. Temperature sensors were mounted at 0.05, 0.10, 0.20, 0.40, 0.60, 0.80, 1.10, 1.45, 1.85, and 2.25 m height. In addition, air temperature was measured at the inlet and the outlet in order to calculate the normalized temperature using equation (1):

$$K_j = \frac{\theta_j - \theta_s}{\theta_e - \theta_s} \quad (1)$$

Where K_j = normalized temperature at the measured point [-], θ_j = air temperature at the measured point [°C], θ_s = air temperature at the supply inlet [°C], θ_e = air temperature at the exhaust outlet [°C].

Tracer gas measurements were conducted simultaneously with air temperature and velocity measurement. After reaching a steady concentration in the exhaust air, 15 tracer gas measurements were conducted at each point and averaged to evaluate the indoor air quality. It was found that the chamber requires about 40 minutes to reach a steady concentration. The gas monitor was set to a Sample Integration Time of t_{SIT} = 5 seconds, each sampling point required 3.5 minutes per measurement. In order to investigate the vertical gradient of indoor air quality, air was sampled from points at 0.10, 0.60, 1.10, and 1.70 m height. Furthermore, tracer gas concentration was measured at the supply air duct and the exhaust air duct. Ventilation effectiveness index was used to quantify indoor air quality in this research. It was calculated using equation (2):

$$\varepsilon_j = \frac{C_e - C_s}{C_j - C_s} \quad (2)$$

Where ε_j = ventilation effectiveness at the measured point [-], C_e = tracer gas concentration at the exhaust duct [mg/m^3], C_j = tracer gas concentration at the measured point [mg/m^3], C_s = tracer gas concentration at the supply duct [mg/m^3].

CFD simulations

Computational simulations were used to model and simulate a ductless personalized ventilation (DPV) system in the climate chamber. Before running the simulations, the numerical model was validated using results from the empirical measurements. A 3D laser scanner was used to capture the exact geometry of the thermal manikin in order to acquire a better comparison between measured and simulated results (Voelker & Kornadt, 2012). The scanned model was then imported to ANSYS Workbench. DPV was modelled as a pipe with a diameter of 8 cm mounted in front of the occupant. This "pipe" is freestanding, i.e. not connected to a duct or another source of air (see Figure 7). Since REHVA Guidebook reports that the thickness of the first layer of fresh tempered air is 20 cm above the floor when DV is used (Skistad & Mundt, 2002), DPV intake was located 10 cm above the floor. This also complies with the recommendations of Halvoňová and Melikov (2010b). The intake filter suggested by Dalewski et al. (2012) was not modelled since dust and other pollutants on floor level were not counted for during the simulations. DPV outlet was located 40 cm from the manikin's face according to the findings of Kaczmarczyk et al. (2006) which reports that human subjects preferred personalized ventilation systems that were located 30-45 cm in front of the face.

Same boundary conditions used in the empirical measurements were used in the computational simulations. DPV flow rate was set to $\dot{V}_{DPV}$ = 5 and 6.5 l/s, which corresponds respectively to an average target velocity of v = 0.33 and 0.63 m/s at the manikin's face. These settings are based on the recommendations of Bolashikov, Nikolaev, Melikov, Kaczmarczyk, and Fanger (2003), which state that a minimum velocity of 0.3 m/s at the manikin's face is required in order to fully penetrate the thermal plume. Table 1 summarizes the simulated cases in this research. All cases were simulated under climate chamber ventilation rate of $\dot{V}$ = 16, 24, and 43 l/s, and supply air temperature of θ_s = 19°C and 22°C for each ventilation rate.

Table 1: Simulated cases

Case	Description
DV	Displacement ventilation only (reference case)
DPV1	DV combined with Ductless Personalized Ventilation, $\dot{V}_{DPV}$ = 5 l/s
DPV2	DV combined with Ductless Personalized Ventilation, $\dot{V}_{DPV}$ = 6.5 l/s

Thermal comfort and thermal sensation were calculated with the UC Berkeley thermal comfort model using results from the CFD simulations. The UC Berkeley model was also used to investigate the effect of higher relative humidity on the performance of DPV. The model implements a 9-point scale to report the local and overall thermal sensation, in which 4 = very hot, 0 = neutral, and -4 = very cold (Zhang, Arens, Huizenga, & Han, 2010a, 2010c). The model uses a second scale to express local and overall thermal comfort. This scale ranges both upward (where 0 = just comfortable, 4 = very comfortable), and downward (where -0 = just uncomfortable, -4 = very uncomfortable) (Zhang et al., 2010c, 2010b).

Empirical measurements results

Ventilation effectiveness measurements indicate that the ventilation system is creating vertical stratification in which fresh air is in the lower layer of room (Figure 2). This result is expected due to the characteristics of displacement ventilation systems (Skistad & Mundt, 2002). Generally, ventilation effectiveness was higher during when the supply temperature set to θ_s = 19°C. The highest achieved ventilation effectiveness at the breathing level of a sitting occupant (1.1 m from the floor) was ε_j = 0.98 when the chamber was set to *16 l/s_19°C*. This case also resulted the highest indoor air quality gradient between 0.1 and 1.1 m from the floor, in which $\Delta\varepsilon_j$ = 0.23. For a standing person (1.7 m from the floor), the maximum achieved ventilation effectiveness was ε_j = 0.89 during the *24 l/s_19°C* case. When the flow rate of the ventilation system was set to $\dot{V}$ = 43 l/s, ventilation effectiveness was at its minimum at 1.1 m, vertical gradient was at its minimum too. This is due to air mixing caused by high air velocity. Air velocity measurements showed that during the cases in which flow rate $\dot{V}$ = 43 l/s, air velocity reached up to 0.34 m/s at 0.2 m above the floor, which causes a feeling of draft (Skistad & Mundt, 2002). However, when the ventilation system was set to 16 l/s and 24 l/s, the mean air velocity in the chamber was generally low. It never exceeded the limit set by the EN standard for building category II, which is 0.22 m/s for office buildings (EN15251, 2007).

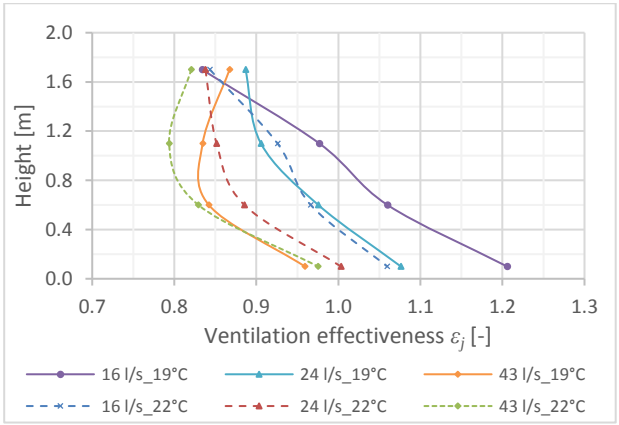

Figure 2: Vertical profiles of ventilation effectiveness

Air temperature measurements show that the vertical air temperature profiles are close when the ventilation rate is set to $\dot{V}$ = 16 and 24 l/s. Yet, at the higher flow rate ($\dot{V}$ = 43 l/s), the vertical profiles became irregular. Similar to the ventilation effectiveness profiles, vertical temperature profiles show relatively small gradient (Figure 3). The largest measured temperature gradient between the height of head and ankle height was 0.6 K/m. This is far lower from the allowed 3 K gradient specified in the ASHRAE standard (ASHRAE, 2009). This indicates that the ventilation system in the climate chamber is promoting air mixing due to high inlet velocity caused by the small cross-section of the supply air inlet (0.01 m^2). This mixing is eliminating the vertical gradient of both temperature and indoor air quality. Therefore, it is inefficient to evaluate the ductless personalized ventilation in the climate chamber using the current ventilation system. Since modifying the ventilation system is highly time and cost consuming, it was decided to use Computational Fluid Dynamics (CFD) simulations to study the performance of the ductless personalized ventilation.

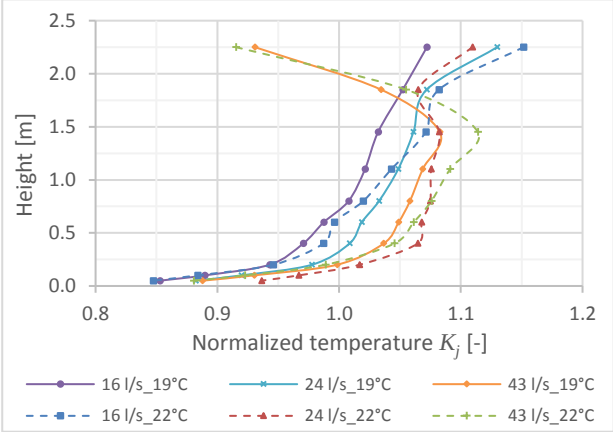

Figure 3: Vertical profiles of air temperature

Simulations results

Validating the numerical model

The numerical model was validated using the data from the empirical measurements that were run under 19°C supply air temperature. ANSYS Fluent was used to solve Reynolds-averaged Navier-Stokes (RANS) equations under steady state. *k-ε* turbulence model was used in this research since it is a simple yet robust model that is widely used to simulate the indoor air movement (Sorensen & Nielsen, 2003). All three *k-ε* models (Standard, Realizable, and RNG) have been used in the literature (Alajmi, Baddar, & Bourisli, 2015; Antoun, Ghaddar, & Ghali, 2016; He et al., 2011; Liu, Liu, Li, & Zuo, 2015; Russo & Khalifa, 2010; Tham & Pantelic, 2010). All three approaches with various settings combinations were tested for this project. It was found that Realizable *k-ε* model with enhanced wall treatment, full buoyancy effects, Green-Gauss Node Based spatial discretization of gradient, and PRESTO! spatial discretization of pressure achieved best agreement with the measured data and reached better convergence. Realizable *k-ε* is usually preferred to Standard *k-ε* since it provides better prediction for spreading rates, recirculation of the flow, and boundary layers under adverse pressure gradients (ANSYS, 2015). A detailed paper is currently being composed by the authors about the validation of a PV numerical model

Buoyancy effects were simulated using the incompressible ideal gas law for air density. Species transport model was used to calculate tracer gas concentrations in the domain. Coupled pressure-velocity scheme was used along with Second Order Upwind scheme to solve the equations of momentum, energy, and species transport.

Modified DV

After the numerical model was validated, a new model was built and the existing ventilation system was optimized by replacing the existing air inlet with a corner mounted quarter-cylindrical supply air terminal with surface area of 0.2 m^2. Furthermore, air outlet was simplified to a 0.1 by 0.45 m rectangular opening. Figure 4 shows a comparison between simulation results of the existing and modified chamber geometry. By comparing the difference in air temperature and ventilation effectiveness between 0.1 m and 1.1 m from the floor, the modified geometry presents a significant increase in the vertical stratification in both air temperature and ventilation effectiveness due to the larger area of the air inlet. This stratification is expected to occur when displacement ventilation is used, and is essential to the performance of the ductless personalized ventilation system. Air temperature difference never exceeded the 3 K limit specified in the ASHRAE standard (2009). Ventilation effectiveness stratification was increased by up to 4.56.

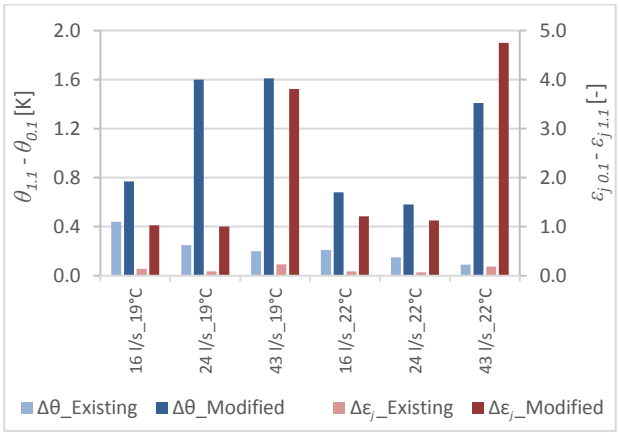

Figure 4: Vertical stratification of air temperature and ventilation effectiveness between simulated existing and simulated modified chamber geometry

CFD results

As shown in Figure 5, the ductless personalized ventilation system reduces air temperature at the face region. This reduction is higher during DPV2 cases, in which the flow rate of the ductless personalized ventilation system is higher. The decrease in air temperature at the face region ranged from $\Delta\theta_{face}$ = -0.4 to -1 K during DPV1 cases. On the other hand, the reduction was $\Delta\theta_{face}$ = -0.7 to -1.4 K during DPV2 cases. This is due to the larger amount of cool air transported from the floor level to the breathing zone. Interestingly, the same pattern did not apply to the difference in indoor air quality, expressed in the ventilation effectiveness index as shown earlier in equation (2). As shown in Figure 6, higher flow rate from the ductless ventilation system did not necessarily mean a better ventilation effectiveness at the face region. In many cases, DPV2 achieved less ventilation effectiveness than DPV1. A possible explanation for this is that higher flow rate of DPV means higher suction at the intake of DPV, which causes more mixing of air around the intake due to high air momentum. However, implementing DPV generally leads to significant improvement of ventilation effectiveness of the breathed air. The improvement of ventilation effectiveness at the face region can be as high as 0.98 when DPV is used compared the reference case of DV alone. Figure 7 shows the effect of ductless personalized ventilation system on air temperature and ventilation effectiveness during DPV1 *24 l/s_22°C* case as an example. It also shows the suction effect of DPV on the lower layer of air above the floor.

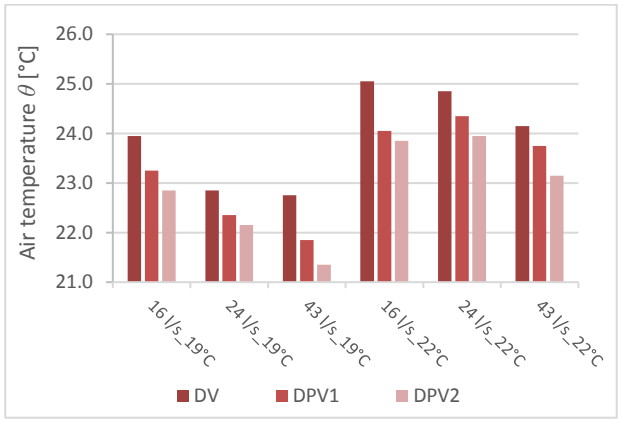

Figure 5: Air temperature at the face region during the simulated cases

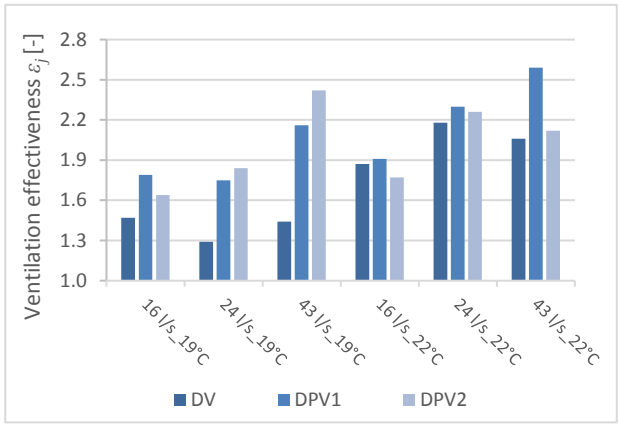

Figure 6: Ventilation effectiveness at the face region during the simulated cases

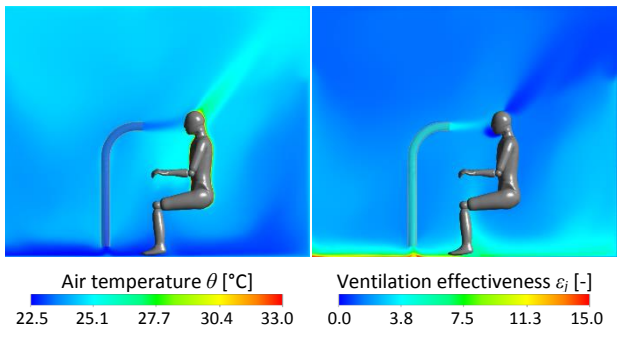

Figure 7: Air temperature (left) and Ventilation effectiveness (right) during DPV1 24 l/s_22°C case

Thermal comfort results

Data acquired from CFD simulations were input into UC Berkeley thermal comfort model in order to investigate thermal sensation and thermal comfort, both overall and local for the 16 body segments defined in the UC Berkeley model. Two cases were selected for investigation using the UC Berkeley model, *16 l/s_19°C* and *16 l/s_22°C*. Each case was simulated under 60% and 85% relative humidity using the same setup cases used in the CFD simulations (DV, DPV1, DPV2). Thus, the investigated cases were *19°C_60%*, *19°C_85%*, *22°C_60%*, and *22°C_85%*.

16 probe points were created in the CFD model around the manikin's geometry to export air temperature and velocity around each body segment to the thermal comfort model. Thermal comfort simulations were run using a time constant model, simulation time was t = 180 minutes for each case. Metabolic heat generation rate was set to 1.2 met to simulate a busy seated occupant in an office (EN13779, 2007).

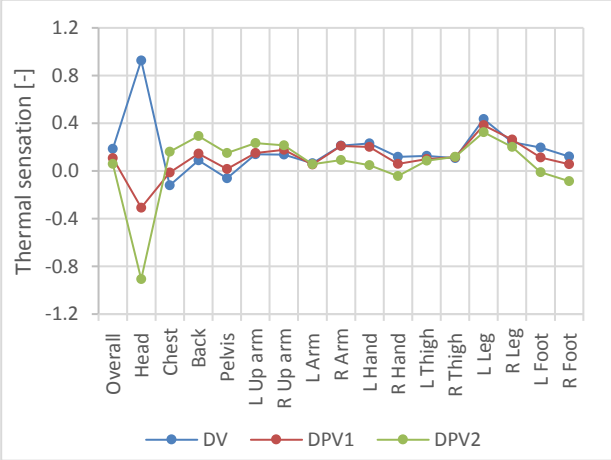

Figure 8: Overall and local thermal sensation during the 22°C_85% case

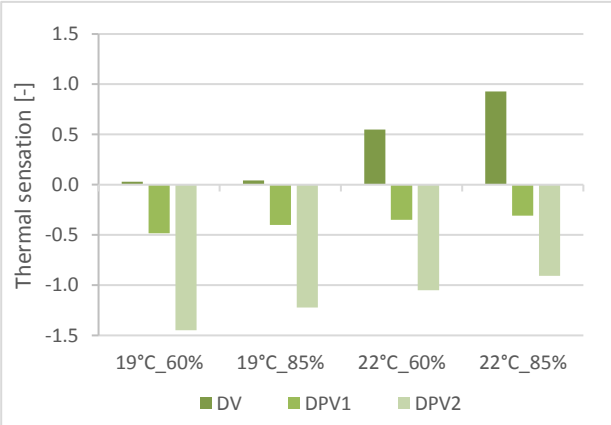

Figure 9: Local thermal sensation at the head during the investigated cases

Results show that the ductless personalized ventilation system always alters the thermal sensation into a lower value on the 9-point scale mentioned in the Methods section of this paper (where 4 = very hot, 0 = neutral, and -4 = very cold (Zhang et al., 2010a, 2010c)). Figure 8 reports the overall and local thermal sensation during the *22°C_85%* case. Even though overall thermal sensation was not drastically changed (-0.08 and -0.13 point with DPV1 and DPV2 respectively), DPV changed the local thermal sensation at the head by up to -1.83 points during the DPV2 setting. Surprisingly, local sensation at some body parts such as chest and back was higher when DPV was implemented. This can be due to redirecting the warm flow of tracer gas from the manikin model's mouth towards the body. The local thermal sensation of other body parts such as hands and feet was colder when DPV was used. This is caused by slight increase in air velocity around these parts, especially the feet, where the suction action of DPV promoted higher air velocity. The other simulated cases resulted similar patterns. Maximum decrease in overall warm thermal sensation was -0.47 point during the *19°C_60%* case.

Figure 9 shows the local thermal sensation at the head during the investigated cases. During the DPV2 cases with supply air temperature of θ_s = 22°C, local thermal sensation reached a maximum limit of -1.05 point. On the other hand, when supply air temperature was θ_s = 19°C, local thermal sensation was up to -1.45 point when the relative humidity was 60%. However, DPV1 had a more subtle effect on local sensation compared to DPV2. It reduced the local thermal sensation at the head to an average of -0.39 point. This suggests that DPV1 was more suitable for the investigated cases since the air temperature at the chamber was generally low due to the lack of heat sources other than the manikin.

Thermal comfort results also indicated promising improvement in some of the simulated cases. Figure 10 shows the overall and local thermal comfort during the *22°C_85%* case. As mentioned earlier in the Methods section, thermal comfort is expressed on a scale that ranges upward (where 0 = just comfortable, 4 = very comfortable), and downward (where -0 = just uncomfortable, -4 = very uncomfortable) (Zhang et al., 2010b, 2010c). Both DPV1 and DPV2 improved the overall thermal comfort by 0.58 point. However, DPV1 had a far better effect on thermal comfort at the head, where local comfort was improved by 2.24 and 1.28 points when using DPV1 and DPV2 respectively. Other body parts experienced slight changes in thermal comfort when the systems were implemented during all of the simulated cases. This is due to minor changes in air temperature and velocity around these parts when DPV1 and DPV2 were used.

Local thermal comfort at the head during all the simulated cases is shown in Figure 11. The system significantly enhanced local thermal comfort during the cases in which supply air temperature was θ_s = 22°C. However, DPV1 showed a better performance than DPV2. When the supply air temperature was set to both 19 and 22°C, DPV2 negatively affected thermal comfort due to the combination of high air velocity with relatively low temperature. DPV1 improved local thermal comfort at the head by only 0.09 point during *19°C_85%* case, and

impaired thermal comfort during the *19°C_60%* case. This suggests that DPV can induce contrary results when the air temperature in the chamber is not uncomfortably high. This effect is more acute with higher flow rates of DPV. This agrees with Melikov's (2004) recommendation of having high PV velocities when the room air temperature is higher than 26°C.

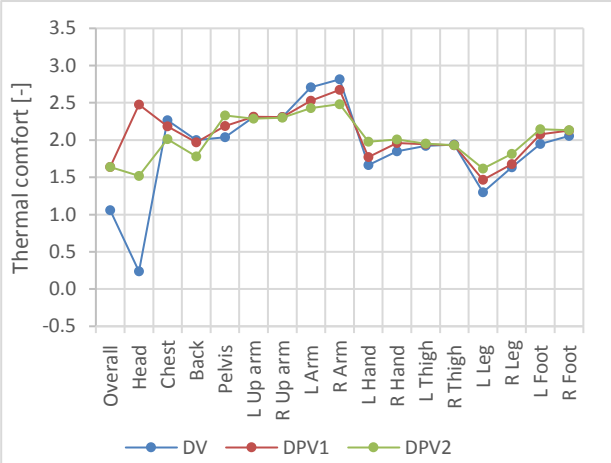

Figure 10: Overall and local thermal comfort during the 22°C_85% case

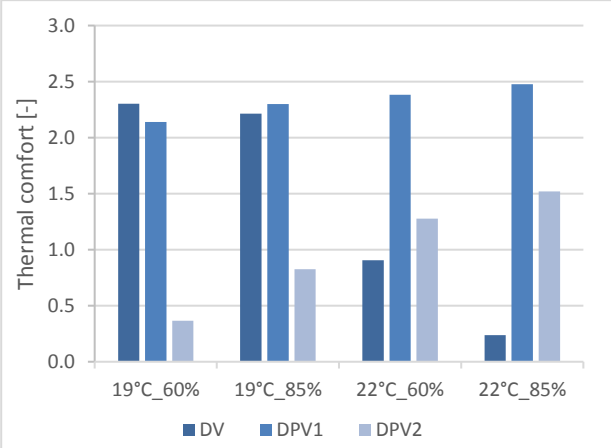

Figure 11: Local thermal comfort at the head during the investigated cases

Conclusions

Computational fluid dynamics simulations show that employing ductless personalized ventilation systems can significantly improve the indoor environment. The system was able to reduce the air temperature at the face by up to 1.4 K when DPV flow rate was set to $\dot{V}_{DPV}$ = 6.5 l/s. Indoor air quality at the face region was also increased when the ductless system was used. DPV increased the ventilation effectiveness index by up to 0.98 compared to the reference case where DPV was not used. However, lower DPV flow rate can improve the inhaled indoor air quality better than higher DPV flow rate due to higher air mixing around the intake.

Results from UC Berkeley thermal comfort model showed that the system can improve overall thermal sensation and local thermal sensation around the head. Furthermore, it can significantly enhance the thermal comfort, both overall and local. However, these results are highly dependent on the air temperature in the room. The system performs better with higher air temperatures and relative humidity. On the contrary, the system can decrease comfort when used with relatively low air temperatures.

Based on the above conclusions, ductless personalized ventilation can be a novel tool to improve the indoor environment. Its flexibility and relatively lower cost give it advantage over the regular ducted personalized ventilation. Further research is currently being conducted to directly compare ducted and ductless personalized ventilation.

Acknowledgement

This research was supported by a scholarship from the Deutscher Akademischer Austauschdienst (DAAD) under the Research Grants – Doctoral Programmes in Germany. Their constant support is highly cherished and appreciated.

References

Abbas, Tariq (1999): Displacement ventilation and static cooling devices: *Building Services Research and Information Association*.

Alajmi, Ali F.; Baddar, Faisal A.; Bourisli, Raed I. (2015): Thermal comfort assessment of an office building served by under-floor air distribution (UFAD) system – A case study. *Building and Environment 85*, pp. 153–159.

ANSYS (2015): ANSYS® Academic Research, Release 16.2, Help System, Coupled Field Analysis Guide. ANSYS, Inc. Available online at www.ansys.com.

Antoun, Sylvie; Ghaddar, Nesreen; Ghali, Kamel (2016): Coaxial personalized ventilation system and window performance for human thermal comfort in asymmetrical environment. *Energy and Buildings 111*, pp. 253–266.

ASHRAE (2009): 2009 ASHRAE Handbook: Fundementals. Atlanta, GA: *American Society of Heating, Refrigeration and Air-Conditioning Engineers*.

Bolashikov, Z.; Nikolaev, L.; Melikov, A. K.; Kaczmarczyk, J.; Fanger, P. O. (2003): New air terminal devices with high efficiency for personalized ventilation application. *In Proceedings of Healthy Buildings 2003* (7), pp. 850–855.

Bolashikov, Zhecho; Melikov, Arsen; Krenek, Miroslav (2010): Control of the Free Convective Flow around the Human Body for Enhanced Inhaled Air Quality. Application to a Seat-Incorporated Personalized Ventilation Unit. *HVAC&R Res. 16* (2), pp. 161–188.

Chakroun, W.; Ghaddar, N.; Ghali, K. (2011): Chilled ceiling and displacement ventilation aided with personalized evaporative cooler. *Energy and Buildings 43* (11), pp. 3250–3257.

Chludzińska, Marta; Bogdan, Anna (2015): The effect of temperature and direction of airflow from the personalised ventilation on occupants' thermal sensations in office areas. *Building and Environment 85*, pp. 277–286.

Conceição, Eusébio Z.E.; Lúcio, Ma. Manuela J.R.; Rosa, Sílvia P.; Custódio, Ana L.V.; Andrade, Renata L.; Meira, Maria J.P.A. (2010): Evaluation of comfort level in desks equipped with two personalized ventilation systems in slightly warm environments. *Building and Environment 45* (3), pp. 601–609.

Dalewski, Mariusz; Melikov, Arsen K.; Vesely, Michal (2014): Performance of ductless personalized ventilation in conjunction with displacement ventilation. Physical environment and human response. *Building and Environment 81*, pp. 354–364.

Dalewski, Mariusz; Vesely, Michal; Melikov, Arsen Krikor (2012): Ductless personalized ventilation with local air cleaning. *In Proceedings of 10th International Conference on Healthy Buildings 2012, Brisbane, Australia 1*.

EN13779 (2007): Ventilation for non-residential buildings – Performance requirements for ventilation and room-conditioning systems; German version EN 13779: *DIN Deutsches Institut für Normung*.

EN15251 (2007): Criteria for indoor environment including thermal, indoor air quality, light and noise. Brussels: *European Committee for Standardization*.

Fanger, P. (2001): Human requirements in future air-conditioned environments. *International Journal of Refrigeration 24* (2), pp. 148–153.

Fanger, Povl Ole (1970): Thermal Comfort: *McGraw-Hill, New York, USA*.

Gao, Naiping; Niu, Jianlei (2004): CFD study on micro-environment around human body and personalized ventilation. *Building and Environment 39* (7), pp. 795–805.

Ghaddar, Nesreen; Ghali, Kamel; Chakroun, Walid (2013): Evaporative cooler improves transient thermal comfort in chilled ceiling displacement ventilation conditioned space. *Energy and Buildings 61*, pp. 51–60.

Halvoňová, Barbora; Melikov, Arsen K. (2010a): Performance of "ductless" personalized ventilation in conjunction with displacement ventilation. Impact of disturbances due to walking person(s). *Building and Environment 45* (2), pp. 427–436.

Halvoňová, Barbora; Melikov, Arsen K. (2010b): Performance of "ductless" personalized ventilation in conjunction with displacement ventilation. Impact of intake height. *Building and Environment 45* (4), pp. 996–1005.

He, Qibin; Niu, Jianlei; Gao, Naiping; Zhu, Tong; Wu, Jiazheng (2011): CFD study of exhaled droplet transmission between occupants under different ventilation strategies in a typical office room. *Building and Environment 46* (2), pp. 397–408.

Kaczmarczyk, J.; Melikov, A.; Bolashikov, Z.; Nikolaev, L.; Fanger, P. O. (2006): Human Response to Five Designs of Personalized Ventilation. *HVAC&R Res. 12* (2), pp. 367–384.

Kalmár, Ferenc; Kalmár, Tünde (2013): Alternative personalized ventilation. *Energy and Buildings 65*, pp. 37–44.

Lipczynska, Aleksandra; Kaczmarczyk, Jan; Melikov, Arsen K (2014): Performance of radiant cooling ceiling combined with personalized ventilation in an office room: identification of thermal conditions. *In Proceedings of 13th International Conference on Indoor Air Quality and Climate*.

Lipczynska, Aleksandra; Kaczmarczyk, Jan; Melikov, Arsen K. (2015): Thermal environment and air quality in office with personalized ventilation combined with chilled ceiling. *Building and Environment 92*, pp. 603–614.

Liu, Taishun; Liu, Zeqin; Li, Ge; Zuo, Zhenjun (2015): Comparative Study of Numerical Simulation of Indoor Thermal Environment in the Pattern of Personalized Ventilation and Stratum Ventilation. *Procedia Engineering 121*, pp. 785–791.

Melikov, A. K. (2004): Personalized ventilation. *Indoor air 14* (s7), pp. 157–167.

Russo, Jackie S.; Khalifa, H. Ezzat (2010): CFD assessment of intake fraction in the indoor environment. *Building and Environment 45* (9), pp. 1968–1975.

Shen, Chong; Gao, Naiping; Wang, Tingquan (2013): CFD study on the transmission of indoor pollutants under personalized ventilation. *Building and Environment 63*, pp. 69–78.

Skistad, Håkon; Mundt, Elisabeth (2002): Displacement ventilation in non-industrial premises. Brussels: *REHVA, Federation of European Heating and Air-conditioning Associations* (REHVA guidebook, no. 1).

Sorensen, D. N.; Nielsen, P. V. (2003): Quality control of computational fluid dynamics in indoor environments. *Indoor air 13* (1), pp. 2–17.

Tham, Kwok Wai; Pantelic, Jovan (2010): Performance evaluation of the coupling of a desktop personalized ventilation air terminal device and desk mounted fans. *Building and Environment 45* (9), pp. 1941–1950.

Voelker, Conrad; Kornadt, Oliver (2012): Automated coupling of CFD and human thermoregulation

modellingconsidering local climatic parameters. *In Proceedings of the 5th International Building Physics Conference IBPC, Kyoto, Japan*, pp. 945–951.

Wyon, David Peter; Wargocki, Pawel (2006a): Indoor air quality effects on office work. *Creating the productive workplace*, pp. 193–205.

Wyon, David Peter; Wargocki, Pawel (2006b): Room temperature effects on office work: Taylor & Francis London.

Yang, B.; Sekhar, S. C.; Melikov, A. K. (2010): Ceiling-mounted personalized ventilation system integrated with a secondary air distribution system--a human response study in hot and humid climate. *Indoor air* 20 (4), pp. 309–319.

Zeng, Qingfan; Zhao, Rongyi (2005): Prediction of perceived air quality for personalized ventilation systems. *Tsinghua Science & Technology 10* (2), pp. 227–232.

Zhang, Hui; Arens, Edward; Huizenga, Charlie; Han, Taeyoung (2010a): Thermal sensation and comfort models for non-uniform and transient environments. Part I: Local sensation of individual body parts. *Building and Environment 45* (2), pp. 380–388.

Zhang, Hui; Arens, Edward; Huizenga, Charlie; Han, Taeyoung (2010b): Thermal sensation and comfort models for non-uniform and transient environments, part II. Local comfort of individual body parts. *Building and Environment 45* (2), pp. 389–398.

Zhang, Hui; Arens, Edward; Huizenga, Charlie; Han, Taeyoung (2010c): Thermal sensation and comfort models for non-uniform and transient environments, part III. Whole-body sensation and comfort. *Building and Environment 45* (2), pp. 399–410.